Commun. Theor. Phys. (Beijing, China) **45** (2006) pp. 437–446

Vol. 45, No. 3, March 15, 2006

Associated Productions of HZZ and HHZ at Linear Colliders in Large Extra Dimension Model*

ZHOU Ya-Jin, MA Wen-Gan, HAN Liang, ZHANG Ren-You, and JIANG Yi

Department of Modern Physics, University of Science and Technology of China, Hefei 230026, China

(Received July 20, 2005)

Abstract *In this paper we investigate the effects of the large extra dimensions on the two processes $e^+e^- \to H^0Z^0Z^0$ and $e^+e^- \to H^0H^0Z^0$ at linear colliders in both unpolarized and polarized collision modes. We find that the virtual Kaluza–Klein graviton exchange can significantly enhance the cross section from their standard model expectations for these two processes. The results show that the LED effect on the process $e^+e^- \to H^0Z^0Z^0$ allows the observation limits on the effective scale M_S to be probed up to 9.75 TeV and 10.1 TeV in the unpolarized and $+-(\lambda_{e^+} = 1/2, \lambda_{e^-} = -1/2)$ polarized beam collision modes (with $\mathcal{P}_{e^+} = 0.6$, $\mathcal{P}_{e^-} = 0.8$), respectively. For the process $e^+e^- \to H^0H^0Z^0$, these limits on M_S can be probed up to 6.06 TeV and 6.38 TeV in the unpolarized and polarized collision modes separately. We find that the $\lambda_{e^+} = 1/2$, $\lambda_{e^-} = -1/2$ polarization collision mode in both process $e^+e^- \to H^0Z^0Z^0$ and $e^+e^- \to H^0H^0Z^0$ may provide a possibility to improve the sensitivity in probing the LED effects.*

PACS numbers: 04.50.+h, 11.10.Kk, 12.60.-i, 13.66.Fg
Key words: large extra dimensions, linear collider, Higgs boson, gauge boson

1 Introduction

Although the Standard Model (SM) has been proved to be a very successful theory below TeV scale, it still has some unsolved problems, such as the hierarchy problem. The idea that there exist large extra dimensions (LED)[1] might provide a solution to the hierarchy problem. In the LED theory there is only one fundamental energy scale M_S for particle interactions, which is of the order of TeV, to solve the hierarchy problem. The usual Planck scale $M_P = 1/\sqrt{G_N} \sim 1.22 \times 10^{19}$ GeV (where G_N is Newton's constant) is related to M_S by the equation in $(4+n)$ dimensions,[2]

$$M_P^2 \sim R^n M_S^{2+n}\,, \tag{1}$$

where n is the number of extra dimensions, and R is the radius of the compactified space.

If we set $M_S \sim 1$ TeV, we can calculate the value of R from Eq. (1). For $n = 1$, we have $R \sim 10^{13}$ cm, which is obviously ruled out by current gravitational observations. For $n \geq 2$, there exists $R < 1$ mm. Since we have not probed gravity at distances smaller than a millimeter, the astro-physical constraints from supernova cooling and cosmic diffuse gamma radiation tell us that $n = 2$ must be ruled out too.[3] When $n \geq 3$, where $R \sim 1$ nm, it is possible to detect graviton signal at high energy colliders.

The large extra dimension model becomes an attractive extension of the SM because of its possible testable consequences. As Arkani-Hamed, Dimopoulos, and Dvali[1] proposed, the SM particles exist in the usual (3+1)-dimensional space, while graviton propagates in a higher-dimensional space. A massless graviton propagating in D-dimensions is equivalent to the picture of numerous massive Kaluza–Klein gravitons propagating in 4 dimensions. In both processes with real graviton emission and the virtual graviton exchange, we should make an incoherent sum over the tower of graviton modes. The summation over these numerous KK graviton states can compensate the suppression factor of $1/M_P$, which appears in the gravitational interactions in the 4 spacetime dimensions.[2,4] Therefore, we can obtain a near electroweak interaction strength for the interactions involving graviton, and it would be possible to discover the LED effects experimentally.

The most frequently discussed processes with virtual KK graviton exchange are two-body final state processes, such as $f\bar{f} \to \gamma\gamma$,[2] $\gamma\gamma \to W^+W^-$,[5] and $e^+e^- \to f\bar{f}$, $q\bar{q} \to l^+l^-$, $gg \to l^+l^-$.[6] Once the KK graviton is discovered, we should consider its effect on more complicated processes. Recently, the studies of the LED effects have been extended to three-body final state processes. For example, the $t\bar{t}H$ associated production at LC can be used to probe the Yukawa coupling and the LED effects.[7,8] $e^+e^- \to H^0H^0Z^0$ is also an important process in testing Higgs self-coupling.[9,10] In Ref. [11] the authors have calculated the LED effect for processes $e^+e^- \to H^0H^0Z^0$ and $e^+e^- \to H^0H^0\gamma$ in unpolarized e^+e^- collision mode, and give the result that for $n = 3$ and $m_H = 120$ GeV at a $\sqrt{s} = 3$ TeV linear collider. The fundamental Planck scale M_S can be probed up to 6.6 TeV and 7.4 TeV respectively. There is another important process $e^+e^- \to H^0Z^0Z^0$ in probing the Higgs coupling with gauge boson,[12] and the detailed information of the Z^0 bosons in the final state is

*The project supported in part by National Natural Science Foundation of China and the Special Fund of the Chinese Academy of Sciences

easy to obtain in the experiment.

In this paper we assume that the Higgs boson had already been discovered and its mass determined. We calculate the LED effect for the $e^+e^- \to H^0Z^0Z^0$ process and consider the $e^+e^- \to H^0H^0Z^0$ process with different polarization colliding beams. The paper is arranged as follows. In Secs. 2 and 3, we present the analytical calculation, the numerical results, and some discussion for the two processes respectively. Finally, a short summary is given.

2 Analytical Calculations

In this section we give the analytical calculations of the processes $e^+e^- \to H^0Z^0Z^0$ and $e^+e^- \to H^0H^0Z^0$ with different polarizations of colliding beams in the LED model. In our calculation we use the de Donder gauge.

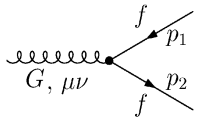

$$C_{ffG} = -\mathrm{i}\tfrac{\kappa}{8}\,[\gamma_\mu(p_1+p_2)_\nu + \gamma_\nu(p_1+p_2)_\mu - 2\eta_{\mu\nu}(\not{p}_1 + \not{p}_2 - 2m_f)]$$

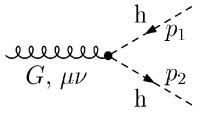

$$C_{hhG} = \mathrm{i}\,\kappa(B_{\mu\nu\alpha\beta}p_1^\alpha p_2^\beta - \tfrac{1}{2}\eta_{\mu\nu}m_h^2)$$

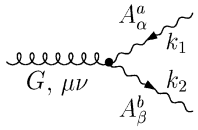

$$C_{AAG} = \mathrm{i}\kappa[B_{\mu\nu\alpha\beta}m_A^2 + (C_{\mu\nu\alpha\beta\rho\sigma} - C_{\mu\nu\alpha\sigma\beta\rho})k_1^\rho k_2^\sigma]\ \delta^{ab}$$

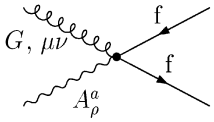

$$C_{ffAG} = \mathrm{i}\,g\tfrac{\kappa}{4}(\gamma_\mu\eta_{\nu\rho} + \gamma_\nu\eta_{\mu\rho} - 2\gamma_\rho\eta_{\mu\nu})T^a$$

Fig. 1 The vertices involving graviton and the corresponding Feynman rules.

In Fig. 1 we present the vertices and Feynman rules which we have used in our calculation, where

$$B^{\mu\nu\alpha\beta} = \frac{1}{2}(g^{\mu\nu}g^{\alpha\beta} - g^{\mu\alpha}g^{\nu\beta} - g^{\mu\beta}g^{\nu\alpha})\,,$$
$$C^{\rho\sigma\mu\nu\alpha\beta} = \frac{1}{2}[g^{\rho\sigma}g^{\mu\nu}g^{\alpha\beta} - (g^{\rho\mu}g^{\sigma\nu}g^{\alpha\beta} + g^{\rho\nu}g^{\sigma\mu}g^{\alpha\beta} + g^{\rho\alpha}g^{\sigma\beta}g^{\mu\nu} + g^{\rho\beta}g^{\sigma\alpha}g^{\mu\nu})]\,,$$
$$\kappa = \sqrt{16\pi G_N}\,. \tag{2}$$

2.1 $e^+e^- \to H^0Z^0Z^0$

The $e^+e^- \to H^0Z^0Z^0$ is an important process in probing the coupling between Higgs and Z^0 bosons, and in Ref. [12] it has been studied in the framework of the SM. Here we give the calculation including the LED effect for this process with different polarizations of incoming beams. We denote this process as

$$e^+(k_1,\lambda_1) + e^-(k_2,\lambda_2) \to H^0(p_1) + Z^0(p_2,\nu) + Z^0(p_3,\mu)\,,$$

where k_i and p_i are the momenta of the incoming and outgoing particles respectively, λ_i is the positron (electron) helicity, and ν and μ are the Lorentz indices of Z^0 bosons. The Feynman diagrams arising from the exchange of KK graviton are shown in Fig. 2.

Here are the amplitudes for these diagrams:

$$\mathcal{M}^G_{(a)}(\lambda_1,\lambda_2) =]\frac{gm_W D(s)P_{\rho\sigma\alpha\beta}}{2S_W C_W(m_H^2 + 2p_1\cdot p_2)}\bar{v}(k_1,\lambda_1)[V_{eeG}]_{\rho\sigma}u(k_2,\lambda_2)[V_{ZZG}]_{\alpha\beta\mu\nu}\ \epsilon_\nu(p_2)\epsilon_\mu(p_3)\,,$$
$$\mathcal{M}^G_{(b)}(\lambda_1,\lambda_2) = \mathcal{M}^G_{(a)}[(p_2,\nu)\leftrightarrow(p_3,\mu)]\,,$$

$$\mathcal{M}^{G}_{(c)}(\lambda_1,\lambda_2)=\frac{-gm_{_W}D(s)P_{\rho\sigma\alpha\beta}}{2S_WC_W^2((p_2+p_3)^2-m_{_H}^2)}\bar{v}(k_1,\lambda_1)[V_{eeG}]_{\rho\sigma}u(k_2,\lambda_2)[V_{HHG}]_{\alpha\beta}\ g_{\mu\nu}\epsilon_\nu(p_2)\epsilon_\mu(p_3)\,, \tag{3}$$

where $s=(k_1+k_2)^2$ is the C.M.S. energy, and

$$D(s)=\frac{16\pi}{\kappa^2}M_S^{-4}\Big(\frac{\sqrt{s}}{M_S}\Big)^{n-2}\Big[\pi+2\mathrm{i}P\int_0^{M_S/\sqrt{s}}\frac{y^{n-1}\,\mathrm{d}y}{1-y^2}\Big]\,,$$
$$P^{\mu\nu\alpha\beta}=\eta^{\mu\alpha}\eta^{\nu\beta}+\eta^{\mu\beta}\eta^{\nu\alpha}-\frac{2}{n-2}\eta^{\mu\nu}\eta^{\alpha\beta}\,. \tag{4}$$

The explicit expressions of vertices V_{eeG}, V_{ZZG}, V_{HHG}, and constant κ are presented in the Eq. (2). The function $D(s)$ represents the summation of the KK excitation propagators.

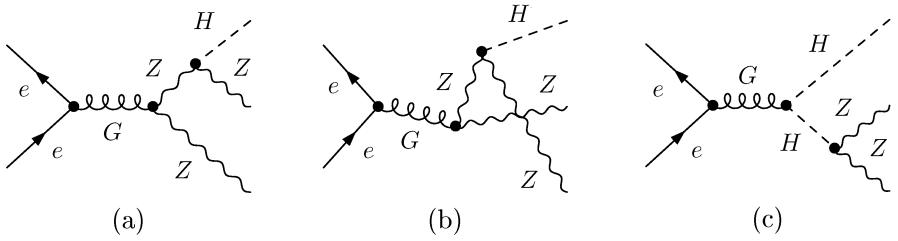

Fig. 2 The tree-level Feynman diagrams with graviton exchange for the process $e^+e^-\to H^0Z^0Z^0$.

We can get the total amplitude after adding these virtual KK graviton exchange amplitudes together with the SM ones. The cross section for unpolarized collision beams in the framework of the LED model is written as

$$\sigma^{\text{unpol.}}_{\text{LED}}=\frac{1}{2}\frac{1}{4|\vec{k}_1|\sqrt{s}}\int\mathrm{d}\Phi_3\frac{1}{4}\sum_{\lambda_1,\lambda_2}|\mathcal{M}(\lambda_1,\lambda_2)|^2\,. \tag{5}$$

The first factor $1/2$ comes from the identical Z^0 bosons in the final states, and the phase-space hypercube element for three final particles process is defined as

$$\mathrm{d}\Phi_3=\Big(\prod_{i=1}^{3}\frac{\mathrm{d}^3\vec{k}_i}{(2\pi)^3 2k_i^0}\Big)\,(2\pi)^4\delta\Big(p_1+p_2-\sum_{j=1}^{3}k_j\Big)\,. \tag{6}$$

In the case of polarization beams, the cross section formula is obtained by the replacement of the following expression in Eq. (5):

$$\sum_{\lambda_1,\lambda_2}|\mathcal{M}(\lambda_1,\lambda_2)|^2\longrightarrow\frac{(1+\mathcal{P}_e)}{2}\frac{(1+\mathcal{P}_p)}{2}|\mathcal{M}(+,+)|^2+\frac{(1+\mathcal{P}_e)}{2}\frac{(1-\mathcal{P}_p)}{2}|\mathcal{M}(+,-)|^2$$
$$+\frac{(1-\mathcal{P}_e)}{2}\frac{(1+\mathcal{P}_p)}{2}|\mathcal{M}(-,+)|^2+\frac{(1-\mathcal{P}_e)}{2}\frac{(1-\mathcal{P}_p)}{2}|\mathcal{M}(-,-)|^2\,, \tag{7}$$

where $\mathcal{P}_e(=(N_e^+-N_e^-)/(N_e^++N_e^-))$ and $\mathcal{P}_p(=(N_p^+-N_p^-)/(N_p^++N_p^-))$ are the polarization efficiency of electron and positron, separately.

2.2 $e^+e^-\to H^0H^0Z^0$

In Ref. [11] the LED effects on the process $e^+e^-\to H^0H^0Z^0$ with unpolarized incoming electron and positron beams have been studied. But the authors did not consider the effect of the linear collider acceptance. Here we will calculate the LED effect of this process with different polarizations of initial states. We denote this process as

$$e^+(k_1,\lambda_1)+e^-(k_2,\lambda_2)\to H^0(p_1)+H^0(p_2)+Z^0(p_3,\mu)\,, \tag{8}$$

where k_i and p_i are the momenta of the incoming and outgoing particles respectively, λ_1 and λ_2 are the positron and electron helicities, and μ is the Lorentz index of Z^0 boson. There are 10 Feynman diagrams contributing to this process, and four of them, which include virtual KK graviton exchange, are shown in Fig. 3. The SM Feynman diagrams and

the corresponding calculations can be found in Ref. [9]

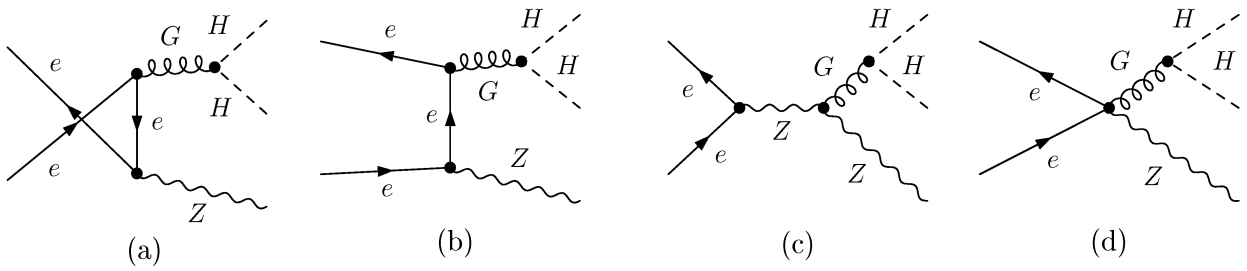

Fig. 3 The tree-level Feynman diagrams with graviton exchange for the process $e^+e^- \to H^0H^0Z^0$.

Here we give the amplitudes for the diagrams shown in Fig. 3:

$$\mathcal{M}^G_{(a)}(\lambda_1,\lambda_2) = \frac{-gD(s_1)P_{\rho\sigma\alpha\beta}}{8C_W(k_1-p_3)^2}\bar{v}(k_1,\lambda_1)\gamma_\mu(1-4S_W^2-\gamma_5)(\not{k}_1-\not{p}_3)[V_{eeG}]_{\rho\sigma}u(k_2,\lambda_2)[V_{HHG}]_{\alpha\beta}\epsilon_\mu(p_3)\,,$$

$$\mathcal{M}^G_{(b)}(\lambda_1,\lambda_2) = \frac{-gD(s_1)P_{\rho\sigma\alpha\beta}}{8C_W(k_2-p_3)^2}\bar{v}(k_1,\lambda_1)[V_{eeG}]_{\rho\sigma}(\not{k}_2-\not{p}_3)\gamma_\mu(1-4S_W^2-\gamma_5)u(k_2,\lambda_2)[V_{HHG}]_{\alpha\beta}\epsilon_\mu(p_3)\,,$$

$$\mathcal{M}^G_{(b)}(\lambda_1,\lambda_2) = \frac{gD(s_1)P_{\rho\sigma\alpha\beta}}{8C_W(s-m_Z^2)}\bar{v}(k_1,\lambda_1)\gamma_\nu(1-4S_W^2-\gamma_5)u(k_2,\lambda_2)[V_{ZZG}]_{\rho\sigma\mu\nu}[V_{HHG}]_{\alpha\beta}\epsilon_\mu(p_3)\,,$$

$$\mathcal{M}^G_{(b)}(\lambda_1,\lambda_2) = \frac{D(s_1)P_{\rho\sigma\alpha\beta}}{2}\bar{v}(k_1,\lambda_1)[V_{eeZG}]_{\rho\sigma\mu}u(k_2,\lambda_2)[V_{HHG}]_{\alpha\beta}\epsilon_\mu(p_3)\,, \tag{9}$$

where $s_1 = (p_1+p_2)^2$. The definitions for notations $D(s)$ and $P_{\rho\sigma\alpha\beta}$ are the same as those in Eq. (4). The total amplitude can be obtained by adding these amplitudes together with the SM ones. The cross section for $e^+e^- \to H^0H^0Z^0$ process in the framework of the LED model can be calculated by using Eqs. (5) $\sim$ (7).

3 Numerical Results

In this section we present some numerical results for the processes $e^+e^- \to H^0Z^0Z^0$ and $e^+e^- \to H^0H^0Z^0$ in both unpolarized and polarized collision modes. In the numerical calculation for polarized beam collision case, we always take the polarization efficiencies of electron and positron beams to be $\mathcal{P}_e = 0.8$ and $\mathcal{P}_p = 0.6$. We assume that the integrated luminosity of electron-positron at LC is $\mathcal{L}_{e^+e^-} = 500$ fb^{-1}. The SM parameters are taken as follows:[13]

$$\alpha(m_z) = \frac{1}{127.918}, \qquad s_w^2 = 0.2312\,,$$
$$m_z = 91.1876 \text{ GeV}\,.$$

To take into account the detecting coverage of the final particles, we take the acceptance angle of electromagnetic calorimeter at the GLC[14] as the acceptance range of Higgs and Z^0 bosons, i.e.,

$$|\cos\theta_{\rm final}| < 0.966\,, \tag{10}$$

where $\theta_{\rm final}$ is the angle between any outgoing particle and the initial electron.

3.1 $e^+e^- \to H^0Z^0Z^0$

In this subsection we give the numerical results of this process in different polarization collision modes with the detecting coverage range of Eq. (10). We use + or − to represent the polarization mode of positron/electron, e.g., +− denote the positron and electron helicities being $\lambda_1 = 1/2$ and $\lambda_2 = -1/2$. From the numerical results, we find that the cross section for ++ or −− polarization collision mode is negligible, at the same time the cross section for +− collision mode is several times larger than that for −+ collision mode. So in the following discussion we only consider the +− polarization collision mode and unpolarization collision mode.

In Fig. 4 we present the cross section for $e^+e^- \to H^0Z^0Z^0$ as functions of colliding energy $\sqrt{s}$ for $n = 3$ and different values of M_S and m_H in unpolarized and +− polarized collision modes, where the electron (positron) polarization efficiency is taken as $\mathcal{P}_e = 0.8$ ($\mathcal{P}_p = 0.6$). We have taken two values of Higgs boson mass, i.e., $m_H = 115$ GeV and $m_H = 180$ GeV. The solid line is for the SM result. The dashed, dotted and dotted-dashed lines are for the cross sections with $M_S = 3.5$ TeV, 4.5 TeV, and 5.5 TeV, respectively. It is obvious that the SM cross section decreases with

the increment of $\sqrt{s}$. When $\sqrt{s}$ is less than about 750 GeV, the LED effect looks very small, but it becomes significant with the increasing of $\sqrt{s}$ due to more virtual KK graviton contributions to the cross section. When $\sqrt{s} = 3$ TeV, the cross section can even exceed 100 fb. We can also see that the cross section for $+-$ polarization collision case is enhanced obviously compared with that in unpolarized collision case.

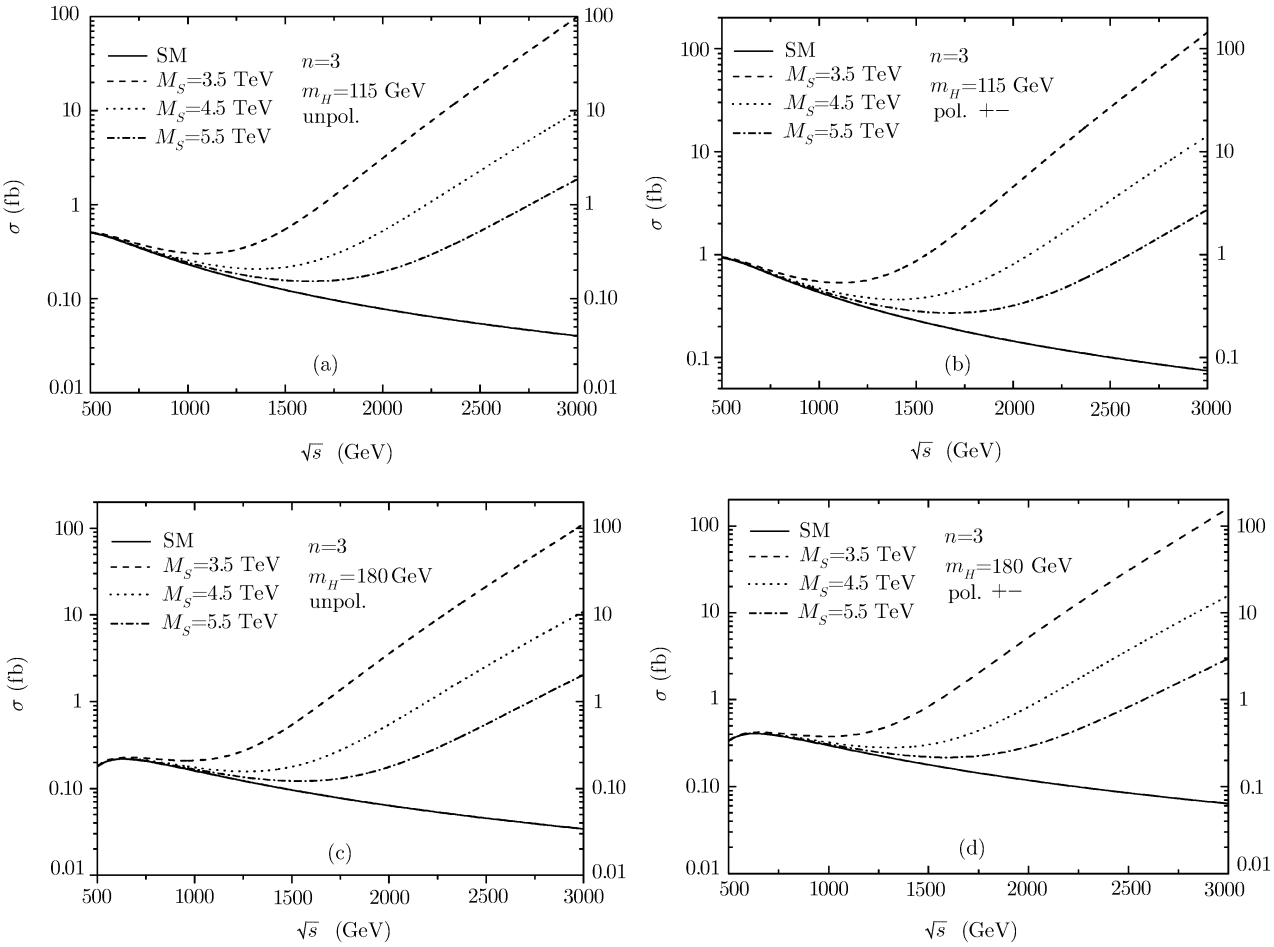

Fig. 4 The dependence of the cross section for $e^+e^- \to H^0Z^0Z^0$ on $\sqrt{s}$. (a) and (c) are for unpolarized e^+e^- collision with $m_H = 115$ GeV and $m_H = 180$ GeV, respectively. (b) and (d) are for $+-$, $\mathcal{P}_e = 0.8$ and $\mathcal{P}_p = 0.6$ polarized e^+e^- collision with $m_H = 115$ GeV and $m_H = 180$ GeV, respectively.

In Fig. 5 we present the dependence of the cross section of the $e^+e^- \to H^0Z^0Z^0$ process on the fundamental scale M_S with $m_H = 115$ GeV or 180 GeV, for unpolarized and $+-$ polarized collision modes. For comparison in different collision energies we take three values of $\sqrt{s}$, which are 1 TeV, 2 TeV, and 3 TeV, respectively. In Figs. 5(a) and 5(b), we depict the results of the cross section with the number of extra dimensions being 3, 4, 5, and 6 respectively. In Figs. 5(a) $\sim$ 5(d) the solid straight lines, which are independent of M_S, are for the SM, the solid curves represent the cross sections for $n = 3$, and the dashed, dotted, and dashed-dotted lines are the cross sections for $n = 4$, 5, and 6 respectively. It is obvious that for a given value of extra dimensions n, the cross section decreases with the increment of M_S, and finally approaches its corresponding SM result. We can see from these figures that the virtual KK graviton contribution decreases with the increment of the value of the extra dimensions n.

To extract the constraint of fundamental energy scale M_S, which can be probed at a future e^+e^- collider, we adopt the same definition of 5σ LED effect observable limit and 3σ exclusion limit with those in Ref. [8], which are

$$\Delta\sigma = \sigma_{\rm LED} - \sigma_{\rm SM} \geq \frac{5\sqrt{\sigma_{\rm LED}\mathcal{L}}}{\mathcal{L}}\,, \tag{11}$$

and

$$\Delta\sigma = \sigma_{\rm LED} - \sigma_{\rm SM} \leq \frac{3\sqrt{\sigma_{\rm LED}\mathcal{L}}}{\mathcal{L}}\,, \tag{12}$$

respectively.

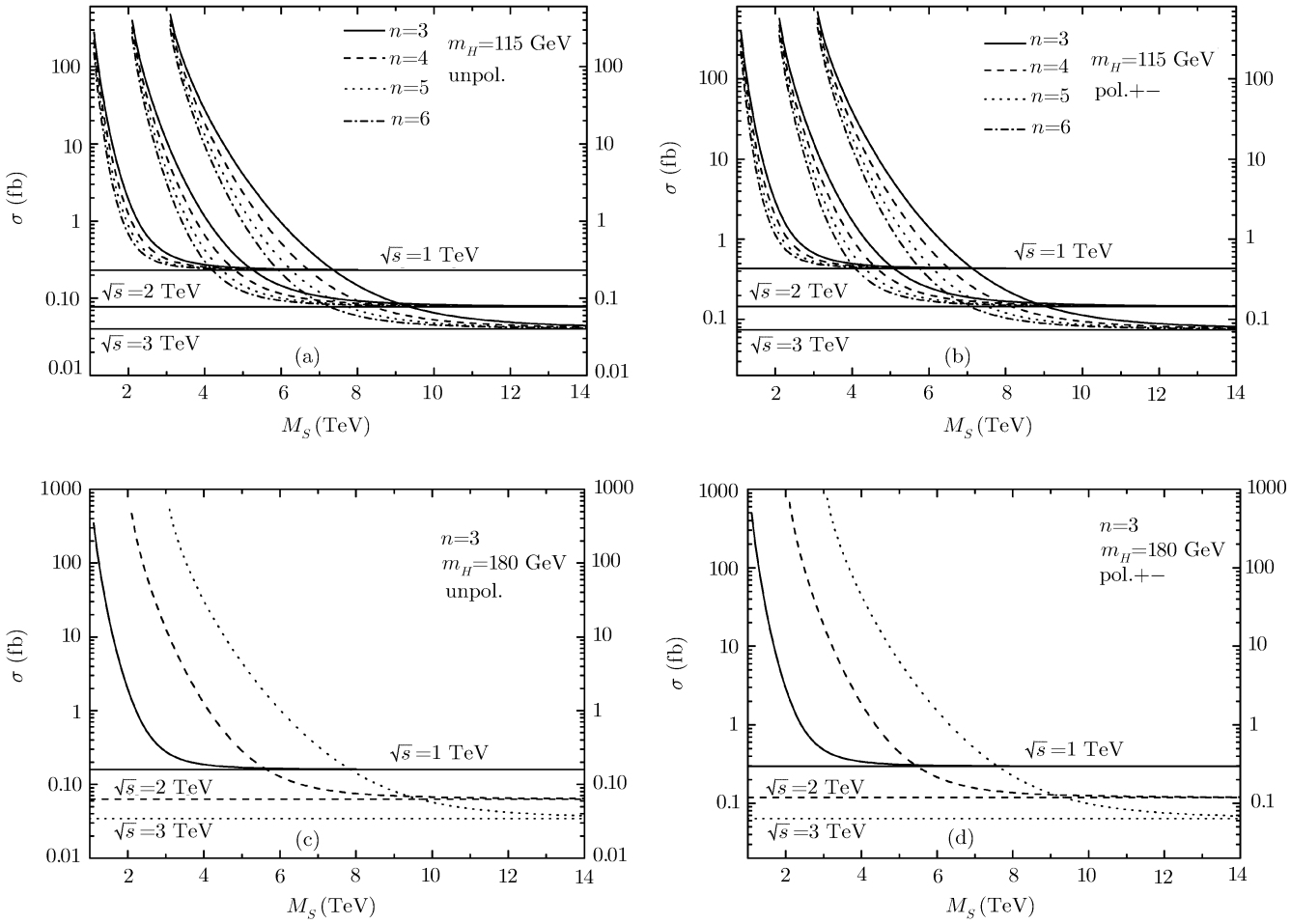

Fig. 5 The dependence of the cross section for $e^+e^- \to H^0Z^0Z^0$ on M_S. (a) and (c) are for unpolarized e^+e^- collision with $m_H = 115$ GeV and $m_H = 180$ GeV, respectively. (b) and (d) are for $+-$, $\mathcal{P}_e = 0.8$ and $\mathcal{P}_p = 0.6$ polarized e^+e^- collision with $m_H = 115$ GeV and $m_H = 180$ GeV, respectively.

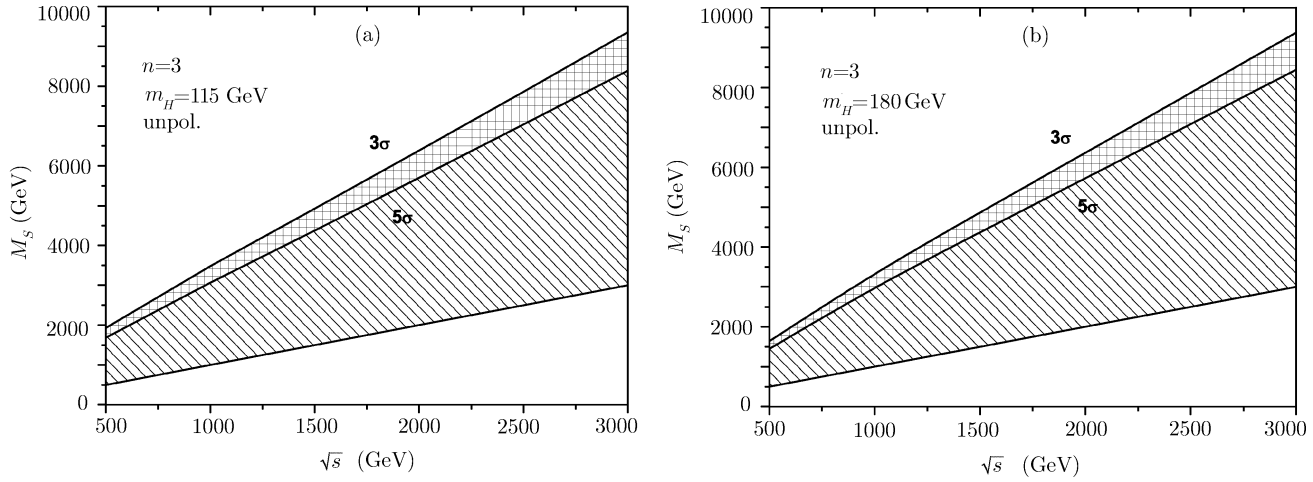

Fig. 6 The LED effect observation area (shadow with oblique lines) and the exclusion area (white) for $e^+e^- \to H^0Z^0Z^0$ process in the $\sqrt{s}$-M_S parameter space with unpolarized beams, where $m_H = 115$ GeV and 180 GeV respectively.

In Fig. 6 we show the regions where the LED effect can and cannot be observed according to Eqs. (11) and (12) in $\sqrt{s}$–M_S parameter space for process $e^+e^- \to H^0Z^0Z^0$ with unpolarized collision beams, with $m_H = 115$ GeV and

180 GeV respectively. The upper white region is the 3σ exclusion region, the oblique lines region is the 5σ observation region, and the underside white region is excluded by the unitary condition $\sqrt{s} < M_S$.

In Table 1, we list the 3σ LED effect exclusion limits and 5σ observation limits with different collision energies $\sqrt{s}$ in both unpolarized and $+-$ polarized collision modes with $m_H = 115$ GeV and 180 GeV respectively. The collision beam polarization efficiencies is also taken to be $\mathcal{P}_p = 0.6$ and $\mathcal{P}_e = 0.8$, and the integrated luminosity is taken as $\mathcal{L}_{e^+e^-} = 500$ fb^{-1}. From this table we can see that the associated $H^0Z^0Z^0$ production process at e^+e^- colliders is a good channel for detecting the LED effect. In the case of $\sqrt{s} = 3.5$ TeV and $m_H = 115$ GeV, the LED effect observation limit on M_S can be probed up to 9.751 TeV (or 10.098 TeV) in unpolarized (or $+-$ polarized) collision mode, while for $\sqrt{s} = 3.5$ TeV and $m_H = 180$ GeV, the LED effect exclusion limit on M_S can be probed up to 10.867 TeV (or 11.214 TeV) in unpolarized (or $+-$ polarized) collision mode. We can see that by using the $+-$ polarized e^+e^- beams, we can improve the sensitivity of probing the LED model effects in $e^+e^- \to H^0Z^0Z^0$ process.

3.2 $e^+e^- \to H^0H^0Z^0$

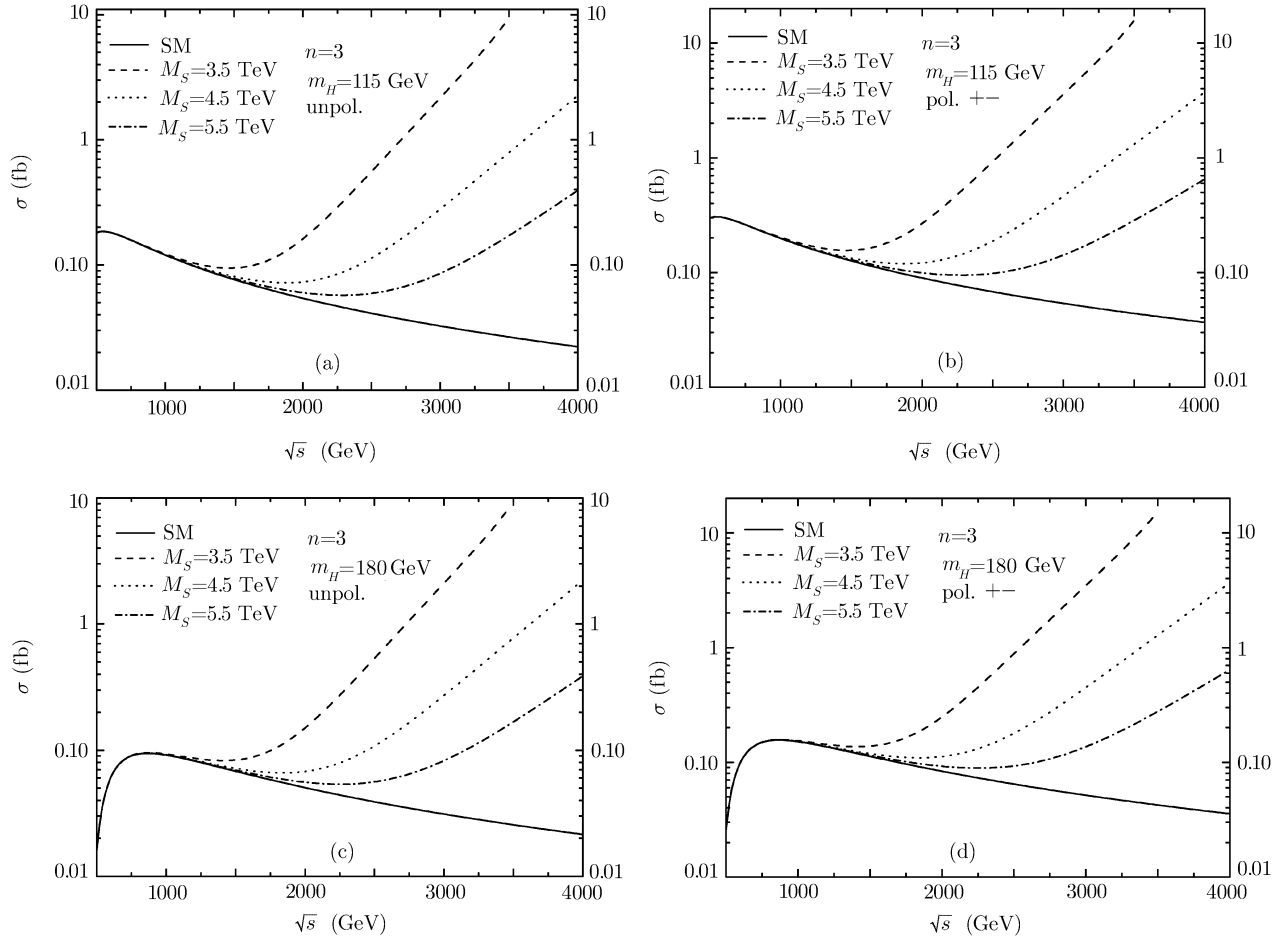

Fig. 7 The dependence of the cross section for $e^+e^- \to H^0H^0Z^0$ on $\sqrt{s}$. (a) and (c) are for unpolarized e^+e^- collision with $m_H = 115$ GeV and $m_H = 180$ GeV, respectively. (b) and (d) are for $+-$, $\mathcal{P}_e = 0.8$ and $\mathcal{P}_p = 0.6$ polarized e^+e^- collision with $m_H = 115$ GeV, and $m_H = 180$ GeV, respectively.

In this subsection we will give the numerical results of $e^+e^- \to H^0H^0Z^0$ process in different polarization collision modes with the final particle acceptance range as shown in Eq. (10). The notations for different polarization modes are the same as those in last subsection. Similar to the calculation of $e^+e^- \to H^0Z^0Z^0$ process, the cross sections for $++$ and $--$ polarization collision modes are almost zero, and the cross section in $+-$ polarization collision mode is several times of that in $-+$ polarization collision mode. We only give the results for unpolarized and $+-$ polarized collision modes in the following discussion. We have checked our calculation for the process $e^+e^- \to H^0H^0Z^0$ in unpolarized collision mode with previous work in Ref. [11], and get coincident results with theirs. But we should notice that in their analysis, they used the relative error of 10% on the cross section measurement to determine 5σ discovery limit

on M_S with the integrated luminosity of 2 ab^{-1}.

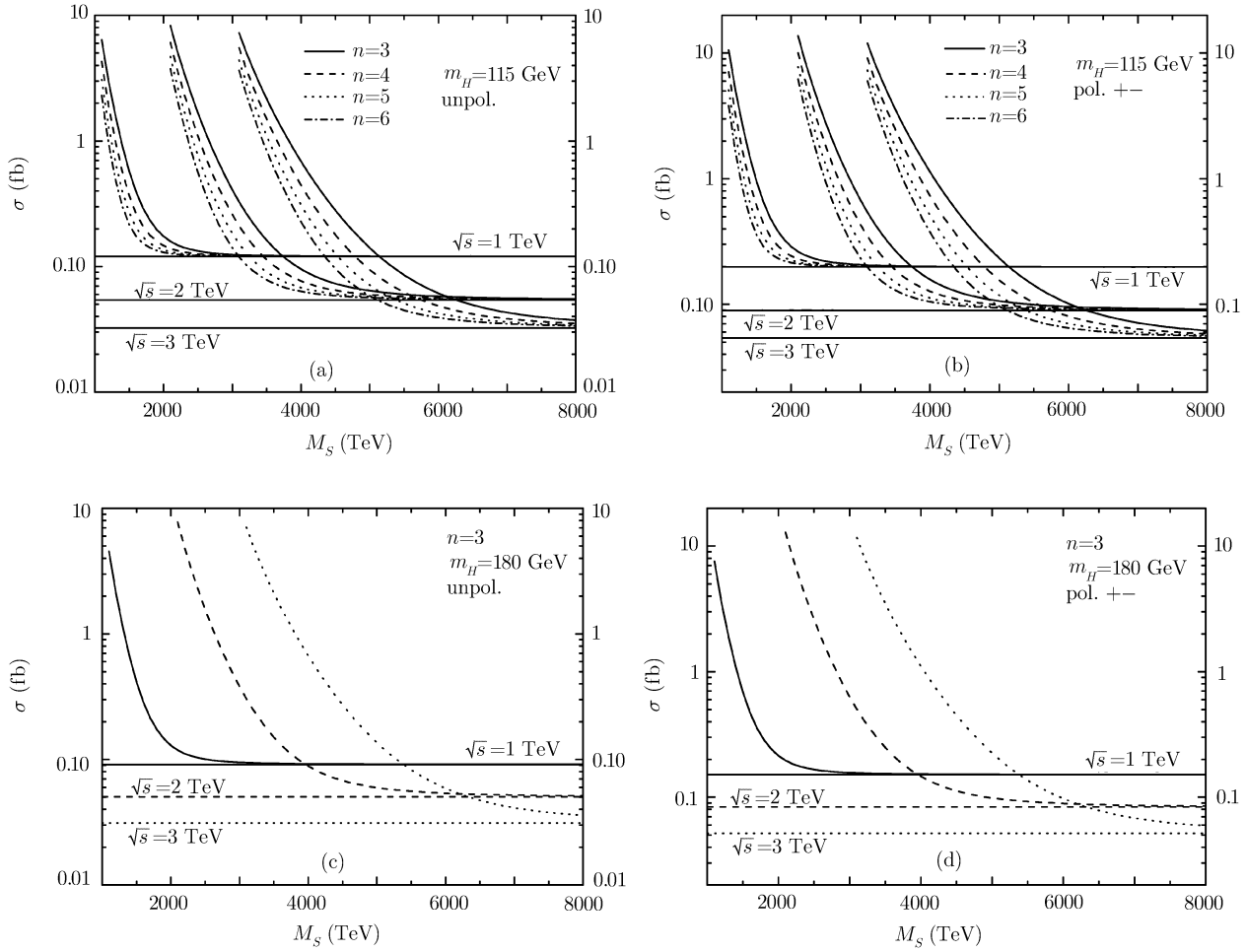

Fig. 8 The dependence of the cross section for $e^+e^- \to H^0H^0Z^0$ on M_S. (a) and (c) are for unpolarized e^+e^- collision with $m_H = 115$ GeV and $m_H = 180$ GeV, respectively. (b) and (d) are for $+-$, $\mathcal{P}_e = 0.8$ and $\mathcal{P}_p = 0.6$ polarized e^+e^- collision with $m_H = 115$ GeV, and $m_H = 180$ GeV, respectively.

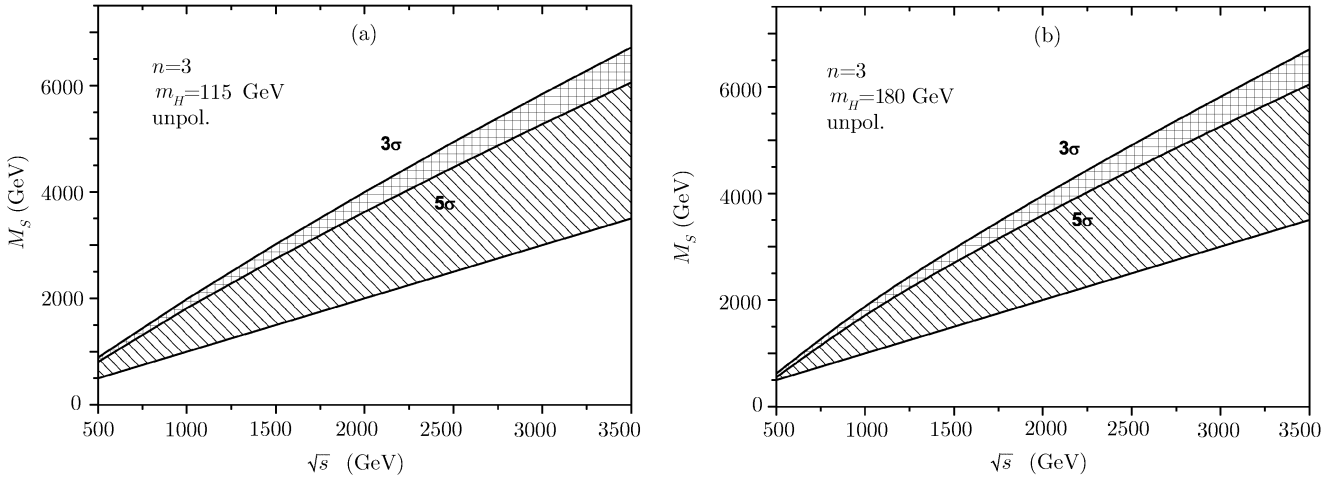

Fig. 9 The LED effect observation area (shadow with oblique lines) and the exclusion area (white) for $e^+e^- \to H^0H^0Z^0$ process in the $\sqrt{s}$–M_S parameter space with unpolarized beams, where $m_H = 115$ GeV and 180 GeV respectively.

Table 1 The 3σ LED effect exclusion limits and 5σ observation limits in the M_S–$\sqrt{s}$ parameter space for the $e^+e^- \to H^0Z^0Z^0$ process. The two tables correspond to $n = 3$, $m_H = 115$ GeV, and 180 GeV, respectively. For the $+-$ polarized e^+e^- collision mode, we set $\mathcal{P}_e = 0.8$ and $\mathcal{P}_p = 0.6$.

$m_H = 115$ (GeV)	M_S (GeV)			
$\sqrt{s}$ (TeV)	unpol.		pol. $+$ $-$	
	3σ	5σ	3σ	5σ
0.5	1930	1683	2029	1771
1.0	3483	3068	3654	3213
1.5	4927	4378	5136	4559
2.0	6383	5700	6623	5917
2.5	7861	7039	8129	7296
3.0	9355	8392	9662	8691
3.5	10867	9751	11214	10098
$m_H = 180$ (GeV)	M_S (GeV)			
$\sqrt{s}$ (TeV)	unpol.		pol. $+$ $-$	
	3σ	5σ	3σ	5σ
0.5	1640	1447	1715	1512
1.0	3355	3000	3485	3111
1.5	4866	4370	5024	4915
2.0	6360	5724	6560	5915
2.5	7862	7079	8098	7316
3.0	9373	8443	9654	8724
3.5	10895	9807	11220	10140

Table 2 The 3σ LED effect exclusion limits and 5σ LED effect observation limits in the M_S–$\sqrt{s}$ parameter space for the $e^+e^- \to H^0H^0Z^0$ process. The two tables are corresponding to $n = 3$, $m_H = 115$ and 200 GeV, respectively. For the $+-$ polarized e^+e^- collision mode, we take $\mathcal{P}_e$=0.8 and $\mathcal{P}_p$=0.6.

$m_H = 115$ (GeV)	M_S (GeV)			
$\sqrt{s}$ (TeV)	unpol.		pol. $+$ $-$	
	3σ	5σ	3σ	5σ
0.5	891	806	935	846
1.0	1988	1816	2076	1899
1.5	3020	2749	3161	2880
2.0	3997	3626	4187	3808
2.5	4935	4465	5172	4694
3.0	5840	5273	6126	5549
3.5	6716	6058	7049	6378
$m_H = 180$ (GeV)	M_S (GeV)			
$\sqrt{s}$ (TeV)	unpol.		pol. $+$ $-$	
	3σ	5σ	3σ	5σ
0.5	623	551	662	585
1.0	1919	1753	2003	1834
1.5	2976	2708	3118	2839
2.0	3965	3598	4152	3777
2.5	4909	4444	5146	4670
3.0	5816	5257	6102	5530
3.5	6697	6045	7033	6364

In Fig. 7 we present the cross sections for $e^+e^- \to H^0H^0Z^0$ as the functions of $\sqrt{s}$ for $n = 3$ with different values of M_S and m_H in unpolarized and $+-$ polarized modes, where the electron (positron) polarization efficiency is taken as $\mathcal{P}_e = 0.8$ ($\mathcal{P}_p = 0.6$). We take two values of Higgs boson mass as $m_H = 115$ GeV and $m_H = 180$ GeV. The solid line is for the SM result. The dashed, dotted, and dotted-dashed lines are corresponding to the cross sections in the LED model for $M_S = 3.5$ TeV, 4.5 TeV, and 5.5 TeV respectively. When $\sqrt{s} < 1$ TeV, the curves for the total cross sections including the LED effect seem to be overlapped with that for the SM, but the LED effect becomes significant with the

increment of $\sqrt{s}$, especially when M_S is not very large. We can also see that the cross section is enhanced obviously after adopting the $+-$ polarization of collision e^-e^+ beams.

In Fig. 8 we present the dependence of the cross section on energy scale M_S for values of $\sqrt{s} = 1$ TeV, 2 TeV, and 3 TeV, with $m_H = 115$ GeV and 180 GeV in unpolarized and $+-$ polarized collision modes, respectively. In Figs. 8(a) and 8(b), we present the curves for the cross sections with the extra dimension n value being 3, 4, 5, and 6 separately. The solid straight lines, which are independent of M_S, are for the SM results, the solid curves are the results for $n = 3$, and the dashed, dotted, and dashed-dotted lines are the cross sections for $n = 4$, 5, and 6 respectively. It is clear that for a given value of n, the cross section decreases rapidly with the increment of M_S, and finally approaches its corresponding SM result. We can see again that the virtual KK graviton exchange contribution decreases with the increment of the n value.

In Fig. 9 we depict the regions where the LED effect can and cannot be observed according to the criteria in Eqs. (11) and (12) in $\sqrt{s}$–M_S parameter space for process $e^+e^- \to H^0H^0Z^0$ in unpolarized beam collision mode, with $m_H = 115$ GeV and 180 GeV respectively. The upper white region is the 3σ LED effect exclusion region, the oblique lines region is the 5σ observation region, and the underside white part is the LED effect excluded region obtained by the unitary condition $\sqrt{s} < M_S$. The integrated luminosity for e^+e^- collider is taken as $\mathcal{L}_{e^+e^-} = 500$ fb^{-1}.

In Table 2, we display the 3σ LED effect exclusion limits and 5σ observation limits with different collision energies $\sqrt{s}$ with $m_H = 115$ GeV and 180 GeV in both unpolarized and $+-$ polarized collision modes respectively. The polarization efficiencies are set to be $\mathcal{P}_p = 0.6$ and $\mathcal{P}_e = 0.8$. We find that both the LED effect exclusion limits and the observation limits will be enhanced after adopting the $+-$ polarized colliding beams, e.g., when $\sqrt{s} = 3.5$ TeV, the LED effect exclusion limit and the observation limit will be increased about 300 GeV. Comparing the results for processes $e^+e^- \to H^0Z^0Z^0$ and $e^+e^- \to H^0H^0Z^0$, we can conclude that in probing the LED effect in an e^+e^- linear collider, the process $e^+e^- \to H^0Z^0Z^0$ may be more sensitive than the process $e^+e^- \to H^0H^0Z^0$, especially in the $+-$ polarization collision mode. In the process $e^+e^- \to H^0Z^0Z^0$ the upper limits of M_S to be observed can be 9.751 TeV and 10.098 TeV for $n = 3$, $\sqrt{s} = 3.5$ TeV and $m_H = 115$ GeV in unpolarized and $+-$ polarized (with $\mathcal{P}_p = 0.6$ and $\mathcal{P}_e = 0.8$) collision modes respectively.

4 Summary

In this paper we studied the processes $e^+e^- \to H^0Z^0Z^0$ and $e^+e^- \to H^0H^0Z^0$ in the framework of large extra dimensions model. We considered different polarization collision modes at electron-positron linear colliders in our calculation. We investigated the 5σ LED effect observation limits and the 3σ LED effect exclusion limits in the M_S–$\sqrt{s}$ parameter space for these two processes. We find that for the process $e^+e^- \to H^0Z^0Z^0$ with $n = 3$, $m_H = 115$ GeV and $\sqrt{s} = 3.5$ TeV, the 5σ observation limits on the fundamental scale M_S can be probed up to 9.75 TeV and 10.1 TeV in the unpolarized and $+-$ (with $\mathcal{P}_{e^+} = 0.6$, $\mathcal{P}_{e^-} = 0.8$) polarized collision modes, respectively. For the process $e^+e^- \to H^0H^0Z^0$ with $n = 3$, $m_H = 115$ GeV, and $\sqrt{s} = 3.5$ TeV, the 5σ LED effect observation limits on M_S can be probed up to 6.06 TeV and 6.38 TeV in the unpolarized and $+-$ polarized (with $\mathcal{P}_{e^+} = 0.6$, $\mathcal{P}_{e^-} = 0.8$) modes, respectively. We can also see that by using the $+-$ polarized positron-electron (i.e., $\lambda_{e^+} = 1/2$, $\lambda_{e^-} = -1/2$) beams in both processes $e^+e^- \to H^0Z^0Z^0$ and $e^+e^- \to H^0H^0Z^0$, the sensitivity of probing the LED effects can be significantly improved.

References

[1] N. Arkani-Hamed, S. Dimopoulos, and G.R. Dvali, Phys. Lett. B **429** (1998) 263, arXiv:hep-ph/9803315; I. Antoniadis, N. Arkani-Hamed, S. Dimopoulos, and G.R. Dvali, Phys. Lett. B **436** (1998) 257, arXiv:hep-ph/9804398.

[2] G.F. Giudice, R. Rattazzi, and J.D. Wells, Nucl. Phys. B **544** (1999) 3, arXiv:hep-ph/9811291.

[3] S. Cullen and M. Perelstein, Phys. Rev. Lett. **83** (1999) 268; L.J. Hall and D. Smith, Phys. Rev. D **60**(1999) 085008.

[4] T. Han, J. Lykken, and R. Zhang, Phys. Rev. D **59** (1999) 105006.

[5] Thomas G. Rizzo, Phys. Rev. D **60** (1999) 115010.

[6] JoAnne L. Hewett, Phys. Rev. Lett. **82** (1999) 4765.

[7] D. Choudhury, N.G. Deshpande, and D.K. Ghosh, JHEP **0409** (2004) 055, arXiv:hep-ph/0311284.

[8] H. Sun, R.Y. Zhang, P.J. Zhou, W.G. Ma, Y. Jiang, and L. Han, Phys. Rev. D **71** (2005) 075005, arXiv:hep-ph/0503183.

[9] A. Djouadi, W. Kilian, M. Muhlleitner, and P.M. Zerwas, Eur. Phys. J. C **10** (1999) 27.

[10] R.Y. Zhang, W.G. Ma, H. Chen, Y.B. Sun, and H.S. Hou, Phys. Lett. B **578** (2004) 349.

[11] N.G. Deshpande and D.K. Ghosh, Phys. Rev. D **67** (2003) 113006, arXiv:hep-ph/0301272.

[12] M. Baillargeon, F. Boudjema, *et al.*, Nucl. Phys. B **424** (1994) 343.

[13] S. Eidelman, *et al.*, Phys. Lett. B **592** (2004) 1.

[14] Koya Abe, *et al.*, "GLC Project, Linear Collider for TeV Physics", KEK Report 2003-7, September 2003, A/H.